The erbium-impurity interaction and its effects on the 1.54 μm luminescence of Er^{3+} in crystalline silicon

F. Priolo and G. Franzò
Dipartimento di Fisica, Università di Catania, Corso Italia 57, I95129 Catania, Italy

S. Coffa
CNR-IMETEM, Stradale Primosole 50, I95121 Catania, Italy

A. Polman
FOM Institute for Atomic and Molecular Physics, Kruislaan 407, 1098 SJ Amsterdam, The Netherlands

S. Libertino
Dipartimento di Fisica, Università di Catania, Corso Italia 57, I95129 Catania, Italy

R. Barklie and D. Carey
Department of Pure and Applied Physics, Trinity College, Dublin 2, Ireland

(Received 12 April 1995; accepted for publication 1 May 1995)

We have studied the effect of erbium-impurity interactions on the 1.54 μm luminescence of Er^{3+} in crystalline Si. Float-zone and Czochralski-grown (100) oriented Si wafers were implanted with Er at a total dose of $\sim 1\times10^{15}/cm^2$. Some samples were also coimplanted with O, C, and F to realize uniform concentrations (up to $10^{20}/cm^3$) of these impurities in the Er-doped region. Samples were analyzed by photoluminescence spectroscopy (PL) and electron paramagnetic resonance (EPR). Deep-level transient spectroscopy (DLTS) was also performed on p-n diodes implanted with Er at a dose of $6\times10^{11}/cm^2$ and codoped with impurities at a constant concentration of $1\times10^{18}/cm^3$. It was found that impurity codoping reduces the temperature quenching of the PL yield and that this reduction is more marked when the impurity concentration is increased. An EPR spectrum of sharp, anisotropic, lines is obtained for the sample codoped with 10^{20} O/cm^3 but no clear EPR signal is observed without this codoping. The spectrum for the magnetic field **B** parallel to the [100] direction is similar to that expected for Er^{3+} in an approximately octahedral crystal field. DLTS analyses confirmed the formation of new Er^{3+} sites in the presence of the codoping impurities. In particular, a reduction in the density of the deepest levels has been observed and an impurity+Er-related level at $\sim$0.15 eV below the conduction band has been identified. This level is present in Er+O-, Er+F-, and Er+C-doped Si samples while it is not observed in samples solely doped with Er or with the codoping impurity only. We suggest that this new level causes efficient excitation of Er through the recombination of e-h pairs bound to this level. Temperature quenching is ascribed to the thermalization of bound electrons to the conduction band. We show that the attainment of well-defined impurity-related luminescent Er centers is responsible for both the luminescence enhancement at low temperatures and for the reduction of the temperature quenching of the luminescence. A quantitative model for the excitation and deexcitation processes of Er in Si is also proposed and shows good agreement with the experimental results. © *1995 American Institute of Physics.*

I. INTRODUCTION

Erbium doping of crystalline and amorphous silicon has recently attracted enormous interest in view of its potential application in silicon-based optoelectronics.[1–22] Erbium is a rare earth that, in its trivalent charge state, can emit photons at 1.54 μm due to an intra $4f$ shell transition between the $^4I_{13/2}$ and the $^4I_{15/2}$ levels. This emission is particularly attractive since its wavelength falls inside a window of maximum transmission for silica optical fibers. The introduction of Er in Si then makes it possible to couple the optical properties of Er^{3+} with the well-established Si technology. It has been shown[1] that sharp 1.54 μm photoluminescence (PL) can be observed from Er in Si and that this arises from the excitation of Er^{3+} achieved through electron-hole mediated processes. Electroluminescence was also observed in 1985 in an Er-doped Si diode at 77 K.[2] However, in spite of these promising results, the attainment of room-temperature (RT) photo- and electroluminescence (EL) has for a long time been hampered by the effect of a strong temperature quenching. Therefore the Er:Si system has not been considered suitable for optoelectronic applications.

Very recently a renewed interest in Er in Si has been stimulated by the observation that a proper engineering of the Er site in crystalline silicon permits the observation of sharp PL[3,8,14,15,17] and EL[11–13] even at RT. It has been noticed[3–9] that a crucial role in the process is played by the introduction of impurities dispersed in the crystalline Si lattice. In fact, codoping with impurities such as C, F, O, and N, at concentrations of $\sim10^{18}/cm^3$ produces an enhancement of the PL yield at low temperatures. Moreover, as we have shown,[6–9] the incorporation of higher O concentrations (up to $10^{20}/cm^3$) produces several other interesting effects. First of all, the strong Er-O interaction allows the incorporation of

 0021-8979/95/78(6)/3874/9/$6.00

a high Er concentration in Si.[6,9] Second, in the presence of O, the temperature quenching of the 1.54 μm luminescence is strongly reduced.[8] These phenomena are probably associated with a modification in the erbium configuration in presence of the impurity. In fact, extended x-ray-absorption fine structure (EXAFS) analyses[4] have shown that Er in Czochralski (Cz) Si (which contains $\sim 10^{18}$ O/cm^3) is coordinated with 6 oxygen atoms, while in float-zone (FZ) Si (containing $\sim 10^{16}$ O/cm^3) its coordination is with 12 Si atoms. Moreover spreading resistance analyses[7] showed that by increasing the O concentration the fraction of donors associated with Er centers increases by several orders of magnitude.

In the preceding article[19] we have demonstrated that the electronic configuration of the Er:Si system is dramatically modified when oxygen is added. In particular an Er-related level lying 0.15 eV below the conduction band is seen to form as a result of the Er-O interaction. This level might play a key role in the energy transfer between the electronic system of the silicon matrix and the $4f$ shell of the Er ion. The aim of the present article is to study and compare the effects of the Er-impurity interaction in Si for several different impurities (O,C,F). In particular, the temperature quenching of the luminescence, the line shape of the luminescence peak around 1.54 μm, the levels introduced in the Si band gap, and the electron paramagnetic resonance signature are investigated in detail. An analysis of these data allowed us to clarify the role of impurities on the excitation processes of Er^{3+} in silicon.

II. EXPERIMENT

The erbium-impurity interaction in crystalline silicon is studied in the case of O, C, and F by using PL measurements, electron paramagnetic resonance (EPR), and deep-level transient spectroscopy (DLTS). Several sets of samples have been prepared in order to have a constant amount of Er in all of the samples together with (i) a constant concentration of different impurities (C,O,F), (ii) a different concentration of the same impurity (O), (iii) no intentionally coimplanted impurity. Samples for PL analyses have been prepared according to the procedure described below. Wafers of n-type FZ ($\sim$250 Ω cm) and Cz ($\sim$2 Ω cm) Si, (100) oriented, were implanted with Er at 77 K using different ion energies. The total Er fluence was 10^{15}/cm^2. In addition to Er, some of the FZ samples were coimplanted with oxygen or fluorine at different energies in order to produce an almost constant impurity concentration of 1×10^{20}/cm^3 in the Er-doped region. These samples will be hereafter referred to as O doped and F doped, respectively. Alternatively, in some of the Er-doped FZ samples O was introduced at a lower concentration (3×10^{19}/cm^3) in order to study the effect of different O contents. All of these implants produced a continuous amorphous layer. Therefore, after implantation, the samples were annealed at 620 °C for 3 h in order to induce the epitaxial recrystallization of the amorphous layer. Subsequently an additional annealing in a rapid thermal furnace under N_2 flux at 900 °C for 30 s was performed to activate the implanted Er. With this technique we have been able to incorporate Er in good quality crystalline Si with different impurity contents.

In the case of carbon, the technique described above does not work since the epitaxial regrowth is impeded by interfacial instabilities and the interface breaks up with the formation of a twinned material. Therefore we have tried a different approach to incorporate Er (10^{15}/cm^2) and C (a constant concentration of 10^{20}/cm^3) in a good quality single crystal. Instead of amorphizing the samples, we have avoided the amorphization by maintaining the samples at 300 °C during the implantation. After implantation the samples were annealed at 900 °C for 30 s in a N_2 atmosphere to activate the implanted Er. The beneficial role of C in eliminating secondary defects[20] helped in obtaining a good quality single crystal in spite of the hot implants. In fact, transmission electron microscopy (TEM) analyses demonstrated that this sample is a good quality single crystal in which only a few slip lines and dislocation loops are present. This sample will hereafter be referred to as C doped.

PL spectroscopy was carried out using the 514.5 nm line of an Ar^+ laser as a pump source. The pump beam was focused to a 1 mm in diameter spot on the sample and was mechanically chopped at 55 Hz. The PL signal was analyzed with a spectrometer and detected with a liquid-nitrogen-cooled Ge detector. Spectra were recorded using a lock-in amplifier with the chopper frequency as a reference. Low temperature measurements were performed using a liquid-nitrogen-cooled cryostat with the samples kept in vacuum.

Two of the samples were also analyzed by electron paramagnetic resonance (EPR). The measurements were made at a microwave frequency of $\sim$9.23 GHz and the samples were cooled to $\sim$5 K using a He gas flow cryostat.

(DLTS) measurements were performed on samples implanted with Er and codoped with O, C, or F. In order to perform these measurements, we have fabricated p^+-n junctions in n-type doped epitaxial Si layers (7 Ω cm, 22 μm thick) grown on Cz substrates. Er was implanted in these samples at an energy of 5 MeV to a dose of 6×10^{11}/cm^2 so that the Er profile is located in the n-type side of the junction. Multiple O, C, or F implants were performed in order to produce an almost constant impurity concentration of 1×10^{18}/cm^3 in the Er-doped region. For comparison some samples were not codoped with any additional impurity. After implantation the samples were annealed at 900 °C for 30 s under N_2 flux. DLTS measurements were performed by reverse biasing the diode at a voltage of 3 V in order to include the Er profile in the depletion layer. A filling pulse of 1 ms was used.

III. RESULTS AND DISCUSSION

A. Photoluminescence

Figure 1 reports the PL intensity at 1.54 μm for Er in Si containing different O concentrations (a) or different impurities at a constant concentration of 1×10^{20}/cm^3 (b), all as a function of the reciprocal temperature. Data are taken at a constant pump power of 200 mW of the Ar ion laser and refer to samples doped with a constant Er dose of 1×10^{15}/cm^2. The data in Fig. 1(a) show that the Er PL yield

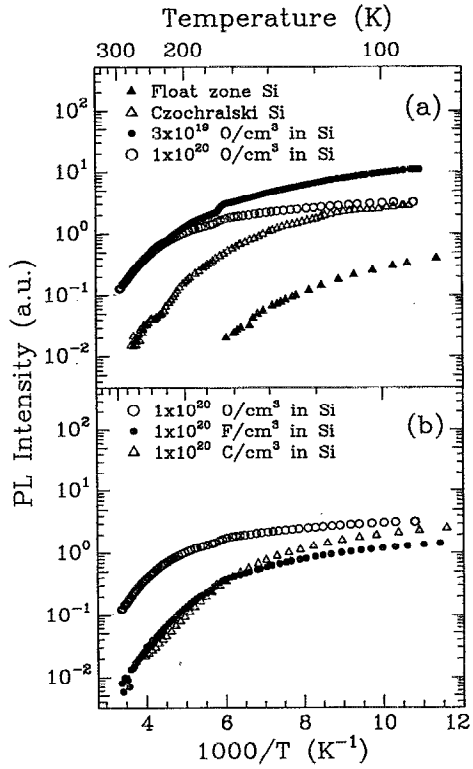

FIG. 1. Photoluminescence intensity at 1.54 μm vs the reciprocal temperature for Er in Si containing (a) different oxygen concentrations; (b) different impurities all at a concentration of 1×10^{20}/cm^3. The total Er dose is in all cases $\sim1\times10^{15}$/cm^2.

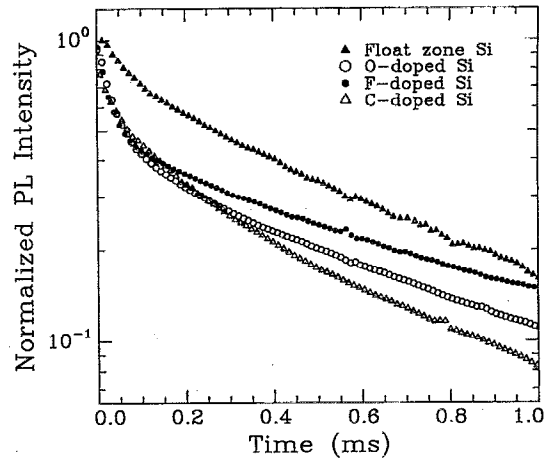

FIG. 2. Time decay of the photoluminescence intensity at 1.54 μm for Er in FZ Si, O-doped Si, C-doped Si, and F-doped Si. Data are taken at 77 K after pumping to steady state at 200 mW and switching off the pumping beam at $t=0$.

at 77 K strongly depends on O concentration. In particular, the yield increases by almost one order of magnitude comparing the FZ sample ($\sim10^{16}$ O/cm^3) to the Cz sample ($\sim10^{18}$ O/cm^3). On further increasing the O concentration, the PL yield first increases (at 3×10^{19} O/cm^3) and eventually decreases. In fact, at 77 K the yield of a sample doped with 10^{20} O/cm^3 is almost identical to that measured in a Cz sample. Therefore for a given Er concentration there seems to exist an optimum O concentration in order to reach maximum PL intensity. This effect has been observed before by Favennec *et al.*[5] in samples coimplanted with Er and O. Since we used solid phase epitaxial regrowth for all of the samples, the effect of different Er:O ratios is compared, in our case, in samples having similar crystal quality, contrary to the work by Favennec *et al.*. A more striking effect of the O codoping is observed on the temperature quenching of the PL. The lowest reduction in the PL yield between 77 and 300 K is observed in the samples intentionally doped with O at 10^{20}/cm^3 (a factor of 30) and 3×10^{19}/cm^3 (a factor of 90). In fact, the two PL curves of these two samples merge in a unique curve above 200 K and a clear RT PL is measured in both samples. In contrast, the PL of Er in Cz-Si decreases more rapidly (a factor of 300) and the PL signal is barely visible at RT. Finally the PL of Er in FZ Si is even more quenched and the signal already falls below the detection limit for temperatures above 180 K. These data demonstrate that higher luminescence intensities at low temperatures not necessarily mean higher intensities also at RT. Indeed the impurity effects on the temperature quenching are very relevant and control RT luminescence.

Similar features are observed in samples codoped with different impurities [Fig. 1(b)]. In fact, the 77 K yield in all of these samples is higher than that observed in FZ samples [see Fig. 1(a)] and the quenching is reduced. Clearly, oxygen is the most efficient species in reducing the temperature quenching, but also F and C have a beneficial effect. In the case of F, the PL intensity is reduced by a factor of $\sim$150 on going from 77 to 300 K and RT PL is still visible. It should be noted that all the curves in Figs. 1(a) and 1(b), except that for the FZ sample, exhibit two rather well-separated regimes. Below $\sim$150 K the PL slowly decreases as the temperature is increased with an activation energy of $\sim$20 meV. At higher temperatures a quenching with an activation energy of $\sim$0.15 eV sets in.

More information on the effect of impurities on the erbium luminescence in Si can be achieved from measurements of the time decay of the luminescence. We have already shown[8] that, in O-doped samples, this decay is not single exponential and consists of a fast decaying component ($\sim$80 μs) and a slow decaying component ($\sim$800 μs). This behavior has been attributed to the existence of at least two different Er sites with different decay channels. Time-decay measurements at 77 K are reported in Fig. 2 for a FZ sample and for the samples codoped with different impurities. It is interesting to note that in all the impurity-rich samples and independent of the impurity type (O, C or F) the decay is not single exponential and consists of a fast and a slow decaying component. The time decay data for the Cz sample and for the sample doped with 3×10^{19} O/cm^3 (not shown) present similar features. On the other hand the FZ sample exhibits an almost single exponential decay characterized by a decay time of $\sim$700 μs. Since this last sample is certainly the one with the lowest impurity content, this observation suggests that the fast decaying component is associated with the pres-

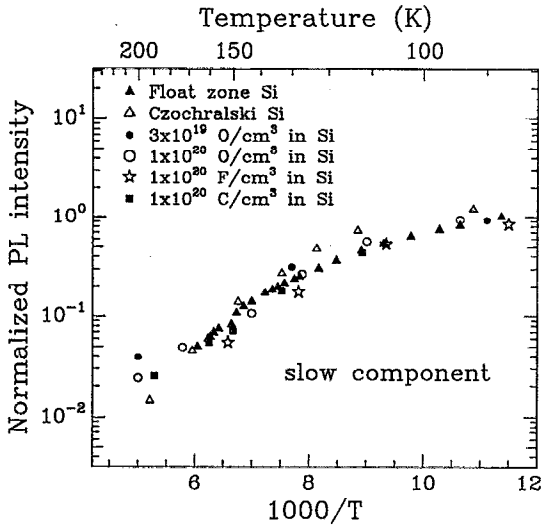

FIG. 3. Temperature dependence of the slow decaying component (~1 ms) of the photoluminescence for Er-doped FZ, Cz, and impurity-doped Si. Data are normalized to the photoluminescence yield of this component at 77 K.

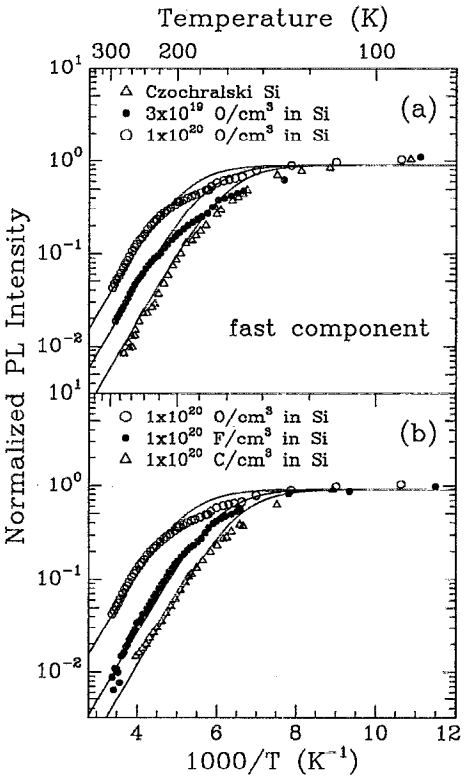

FIG. 4. Temperature dependence of the fast decaying component (~80 μs) of the photoluminescence for Er-doped Si samples with different O contents (a) and with different impurities all at a concentration of 1×10^{20}/cm^3 (b). Data are normalized to the photoluminescence yield of this component at 77 K.

ence of the impurities. All the time-decay curves can be fitted by the sum of two exponentially decaying components. This suggest that two different classes of Er^{3+} ions, having different nonradiative decay routes, are present in these samples. Under this assumption it is possible to decompose from the fits the relative contribution of the fast and slow component. Since decay-time measurements have been performed at different temperatures this decomposition can be repeated at each temperature for the data in Fig. 1. The result of such an exercise is reported in Fig. 3 and Fig. 4 and the data are normalized, for clarity, to the PL intensity at 77 K. The data of Fig. 3 demonstrate that the slow component, which represents about 80% of the total PL intensity in the FZ samples, exhibits an identical quenching behavior in all of the samples independent of the impurity type and concentration. Also the absolute intensities in the different samples are equal within a factor of 2. This component quenches very rapidly with temperature and is no more observable above 200 K.

The quenching behavior of the fast component is radically different. In fact, as shown in Fig. 4, the intensity of this component decreases very slowly below 150 K. At higher temperatures a quenching with an activation energy of 0.15 eV is observed. The temperature at which this regime sets in is, however, dependent on both impurity content [Fig. 4(a)] and codoping species [Fig. 4(b)].

The large effect of impurities in enhancing the contribution of the fast component to the total PL intensity suggests that fast decaying light emission is a signature of Er sites in an impurity-rich environment. On the other hand the data in Fig. 3 suggest that there is always a luminescent Er^{3+} site present in Si, independent of the impurity content, which is characterized by a slow time decay. In FZ Si this is the dominating luminescent site. In impurity-rich samples this site is responsible for part of the low temperature luminescence but plays no role as soon as the temperature is increased above 200 K. Note that since the PL yield at temperatures above 200 K is solely given by the fast component, the 0.15 eV quenching regime must be due to processes occurring at the impurity-rich Er luminescent sites.

The time decay data can all be described by the existence of two different Er sites in crystalline silicon. In the following we will give more evidence of the presence of these sites by means of several analytical techniques.

B. High resolution photoluminescence

The fact that different environments are experienced by Er in the different samples (FZ and impurity-rich samples) can be proven by high resolution PL measurements. In fact, the 1.54 μm transition is dipole forbidden for the free Er ion and, in a solid, it is allowed only because the crystal field will produce a mixture of states with different parity. The extent of the splitting and hence the position and relative intensity of the emission lines will depend significantly on the lattice location of the Er ions and on the chemical environment around it. High resolution (1 nm) spectra taken at 77 K for the different samples are reported in Fig. 5 and clearly show different spectral shapes. In fact the luminescence at ~1.54 μm consists of several peaks, all Er related. Both the relative intensity and exact position of these peaks is strongly dependent on the codoping species. This interesting effect has been noticed before[3,7] and demonstrates that the chemical surrounding of the emitting Er^{3+} centers is different in

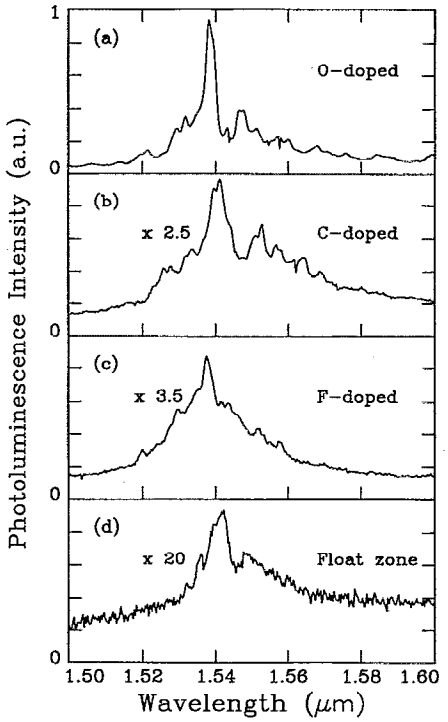

FIG. 5. High resolution photoluminescence spectra at ~1.54 μm for Er in Si containing different impurities. The resolution of these measurements is 1 nm. Spectra were taken at 77 K using a pump beam of 500 mW.

the different samples. It should be noted that the line shape is not only dependent on the codoping species, but also on its concentration. In fact, we[23] have demonstrated that, in the case of oxygen, different O/Er concentration ratios produce different line shapes, while identical O/Er ratios (also by changing the absolute numbers by several orders of magnitude) produce similar line shapes. This is evidence that different emitting Er^{3+} sites do exist and that the specific configuration depends on both codoping species and number of codoping impurities per erbium atom.

C. EPR analyses

Information about the sites occupied by Er^{3+} can also be obtained by EPR. Figure 6 shows the EPR spectrum, in the field range 0.05–0.25 T, obtained for a sample of FZ Si implanted with 1×10^{15} Er/cm^2 and codoped with 1×10^{20} O/cm^3; the magnetic field **B** was parallel to [100] and the sample temperature was ~5 K. The most intense lines labeled 1, 2, 3, and 4 have peak to peak linewidths of 1.2, 1.9, 1.9, and 6.7 mT, respectively, and g values of 10.5, 6.2, and 6.0, and 2.7, respectively; in addition there are other weaker sharp lines. No such spectrum was observed for a sample implanted with 1×10^{15} Er/cm^2 in FZ Si but not codoped with O. Indeed in this latter case no sharp line was detected in the same field range. The spectrum for the O codoped sample exhibits a strong angular dependence as **B** is rotated in the (110) plane: no line has an isotropic g value. Despite the fact that we cannot detect the hyperfine lines arising form the hyperfine interaction with the 22.8% abundant ^{167}Er with

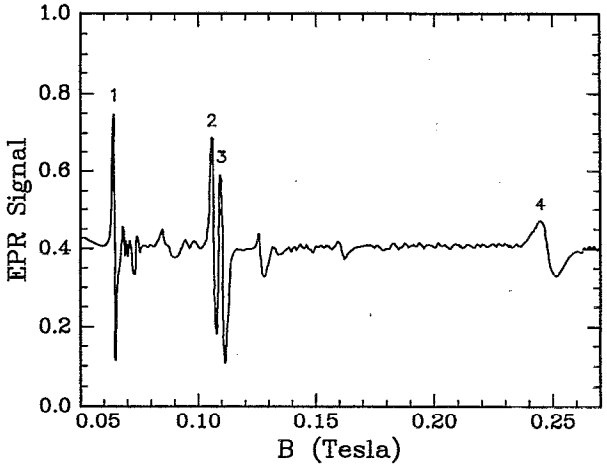

FIG. 6. Electron paramagnetic resonance spectra of Er^{3+} in the O-doped (10^{20}/cm^3) FZ sample which was implanted with 1×10^{15}Er/cm^2. The magnetic field **B** was parallel to the [100] direction and the spectra have been taken at 5 K.

nuclear spin $I=7/2$, it is reasonable to suppose that the lines are associated with Er ions. It is most likely that these Er ions are in the 3+ charge state as the non-Kramers ion Er^{2+} usually has a singlet ground state in a crystal field (at least no resonance from Er^{2+} has ever been detected). The main question to be answered is what is the nature of the site or sites occupied by Er^{3+}. In cubic symmetry the manifold of states with $J=15/2$ is split into two doublets (Γ_6 and Γ_7) and three quartets (Γ_8); the doublets are each associated with isotropic g values [of about (−) 6 and (+) 6.8, respectively] but the Zeeman interaction of the Γ_8 quartets is anisotropic.[24] Er^{3+} ions in GaAs[25,26] and (in site I) in ZnSe[27] occupy sites of tetrahedral symmetry and have an isotropic resonance with $g\sim5.9$ associated with one of the doublets. Although lines 2 and 3 have $g=6.2$ and 6.0 for **B** parallel to the [100] direction, the strong anisotropy of these lines rules out the possibility that they arise from Er^{3+} in Γ_6 or Γ_7 doublets. Er^{3+} in ZnSe (site II)[27] and in MgO[28] does occupy a Γ_8 state as a result of being in an octahedral field arising from an octahedron of Se^{2-} and O^{2-} neighbors, respectively. For **B** parallel to the [100] direction the spectrum for ZnSe:Er^{3+} (site II) has lines at $g=11.53$, 5.596, 2.99, and 2.93 all of which are anisotropic. It is tempting to suppose that the similarity between this spectrum and the spectrum of lines 1–4 (Fig. 6) implies that these lines are also a signature of Er^{3+} in a Γ_8 state arising from the field generated by an octahedron of O^{2-} neighbors. However, although similar, the spectrum is certainly not exactly that expected for such a case. The cause of this discrepancy, whether because (as must be the case for the 1.54 μm light emission) the symmetry is not exactly octahedral or for some other reason, will become clear once the detailed analysis, currently underway, is completed. It is interesting to note that a pseudo-octahedral, nonantisymmetric, site was also suggested on the basis of EXAFS analysis in CZ Si.[4] Finally we note that the other weaker lines in the spectrum of Fig. 6 may arise from Er^{3+} in other different, but well-defined sites.

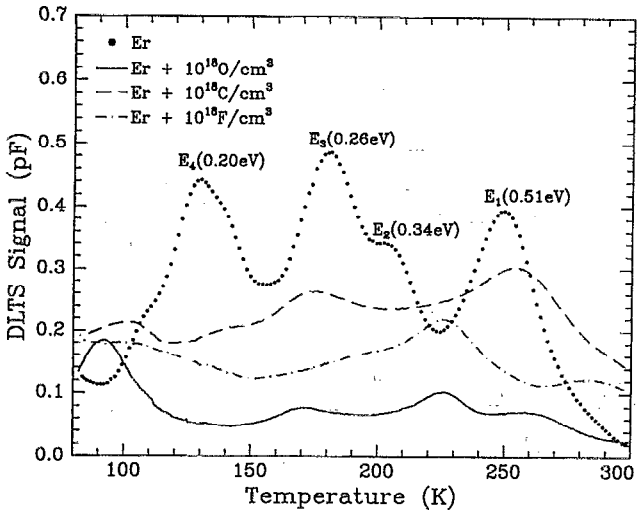

FIG. 7. DLTS spectra of Er in impurity-free, O-doped, C-doped, and F-doped Si. Er was implanted at a dose of $6\times10^{11}/cm^2$. The impurities were all introduced at a concentration of $1\times10^{18}/cm^3$ and the samples were annealed at 900 °C for 30 s.

In summary, our EPR analyses demonstrate that, as a result of the Er-O interaction, new, well-defined Er^{3+} sites have formed.

D. DLTS analyses

The erbium-impurity interactions were also investigated by DLTS analyses. In Fig. 7 we report the DLTS spectra in the temperature range 77–300 K for erbium in impurity-free, O-doped, C-doped, and F-doped Si. Erbium was implanted at a dose of $6\times10^{11}/cm^2$ (corresponding to a peak concentration of $\sim6\times10^{15}/cm^3$) and uniform impurity concentrations at $1\times10^{18}/cm^3$ were realized. A subsequent thermal annealing was performed at 900 °C for 30 s. In impurity-free Er-doped epitaxial Si several DLTS peaks arise, corresponding to levels in the Si band gap with energies E_C-E_T (E_T being the energy of the trap level) of 0.51 eV (E_1), 0.34 eV (E_2), 0.26 eV (E_3), and 0.2 eV (E_4). These levels are not due to the implant damage and have been identified[19] as due to Er-defect complexes. A dramatic change in the spectra is observed when Er and one of the impurities are introduced together in the sample. In all cases, (for O, C, and F) the level structure is modified, demonstrating that a strong interaction between Er and the impurity is occurring. In particular a reduction in the concentration of deep levels is observed and a new peak around 100 K with an activation energy of ~0.15 eV is observed. This peak is not present in the spectra of samples solely implanted with the impurity (O, C, F) and is hence associated with Er-O, Er-F, and Er-C complexes. It is tempting to consider the level at $E_C-0.15$ eV as a signature of the fast decaying luminescent Er^{3+} centers which also are only present in impurity-rich Si and which produce a quenching of the luminescence with an activation energy of exactly 0.15 eV.

E. Discussion

The data reported so far are of major importance in an effort to understand the role of impurities on the Er 1.54 μm luminescence. A few observations are particularly important. Luminescence at 1.54 μm requires Er ions in the 3+ charge state and an efficient energy transfer from the electronic system of the Si matrix to the $4f$ shell of the Er^{3+} ion. In principle impurity doping might either increase the luminescence Er^{3+} population or favor the energy transfer between the matrix and the Er^{3+} ion. Recent theoretical calculations have shown[29] that for Er in Si the optically active 3+ state is by far energetically more favored with respect to the optically inactive 2+ state. On the basis of these calculations we believe that the major role of the impurities is to increase the efficiency of the excitation process. The excitation mechanism of Er^{3+} in Si has been investigated several times.[6,29–31,33] Theoretical calculations[31] have demonstrated that the probability that a band to band electron-hole recombination transfers its energy to the $4f$ shell of Er^{3+} is too small to consider this mechanism plausible. On the other hand, as soon as one of the carriers is localized at an Er-related level, the probability of an Auger recombination exciting the $4f$-shell Er^{3+} electrons increases by several orders of magnitude.[31] Our EPR and DLTS data clearly demonstrate that in the presence of impurities new well-defined Er^{3+} sites form and the bonding character of Er is strongly modified. Indeed DLTS data show that the impurity effect is twofold. First, the spectra clearly show the formation of a new Er-impurity-related level at around 0.15 eV from the Si conduction band. This level is localized on the Er^{3+} ion and might therefore represent a particularly efficient channel among the site and the host. Second, as a result of the impurity-erbium interaction, levels typically lying close to the middle of the Si band gap are strongly reduced. This will of course increase the carrier lifetime and reduce the number of electron-hole recombinations not ending up with an erbium excitation (with a beneficial effect on the 1.54 μm luminescence). In Sec. IV we will show that the modifications produced in the Er configuration can quantitatively account for the impurity effect on the PL yield at low temperatures and on the temperature quenching of the PL.

IV. EXCITATION MECHANISM

It has been recently shown[32,33] by time resolved spectroscopy that after a short pumping laser pulse the excitation of Er^{3+} ions continues for times as long as 50 μs at 4 K. Since the excess carriers generated by the laser are expected to have a lifetime much shorter than 50 μs in Er-doped samples, this interesting observation suggests that Er^{3+} excitation involves carriers localized at an Er-related level. The excitation can for example occur through the recombination of e-h complexes bound to this level. In this picture the 50 μs are associated with the lifetime of these complexes. The proposed excitation mechanism can be the one sketched in Fig. 8. The gateway for the energy transfer is an Er-related level. We assume that the level is a donor and becomes neutral by capturing an electron. This level can still bind a hole as a consequence of the large strain produced by the

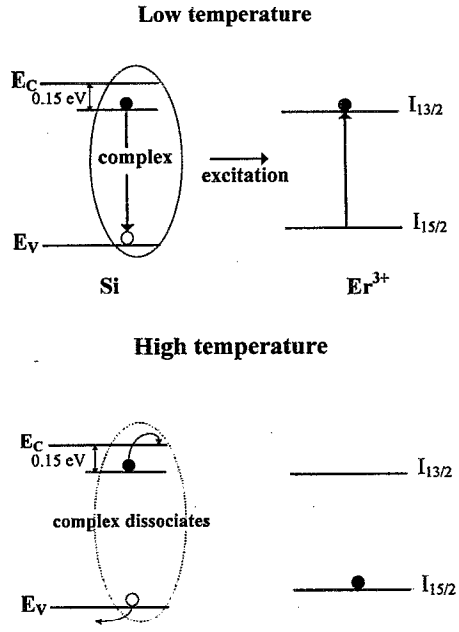

FIG. 8. Schematic picture of the excitation mechanism of Er^{3+} in Si.

impurity-Er complex. While the hole is trapped, recombination of the e-h complex with energy transfer to the Er ion can occur. However, if the electron is thermalized to the conduction band, the center becomes positively charged and the Coulomb repulsion immediately produces the detrapping of the hole. If thermalization occurs before the energy transfer takes place, the effective excitation rate through this mechanism will be severely reduced. The carrier thermalization will become increasingly important when the temperature is increased [see Fig. 8(b)].

The intensity of the PL is proportional to the concentration of Er^{3+} ions which are excited, i.e.,

$$I \propto \frac{N_{\mathrm{Er}}^*}{\tau_{\mathrm{rad}}} \tag{1}$$

with N_{Er}^* the concentration of excited erbium ions and τ_{rad} the radiative lifetime. When most of the Er is not excited ($N_{\mathrm{Er}}^* \ll N_{\mathrm{Er}}$) the concentration of excited erbium ions is given by

$$\frac{dN_{\mathrm{Er}}^*}{dt} = \frac{n_C}{\tau_{\mathrm{tr}}} - \frac{N_{\mathrm{Er}}^*}{\tau}, \tag{2}$$

where n_C is the concentration of e-h complexes, τ_{tr} is the time required for energy transfer, and τ the decay lifetime of the Er luminescence. At steady state

$$N_{\mathrm{Er}}^* = \frac{n_C}{\tau_{\mathrm{tr}}}\tau \tag{3}$$

and hence the luminescence intensity will be given by

$$I \propto \frac{N_{\mathrm{Er}}^*}{\tau_{\mathrm{rad}}} = \frac{n_C}{\tau_{\mathrm{tr}}}\frac{\tau}{\tau_{\mathrm{rad}}}. \tag{4}$$

The concentration n_C is determined by the following rate:

$$\frac{dn_C}{dt} = R_C - R_D - R_E, \tag{5}$$

where $R_C = \sigma_p v_{\mathrm{th}} p f(E_T)(N_{\mathrm{Er}} - n_C)$ is the formation rate of the complexes, with σ_p the cross section for hole capture, v_{th} the hole thermal velocity, p the hole concentration, $f(E_T)$ the probability that the level is occupied by an electron, and N_{Er} the concentration of Er ions that introduce in the gap the level E_T; $R_D = e_n n_C$ is the dissociation rate of the complexes, with e_n the emission rate to the conduction band for an electron localized at the center (it is assumed that thermalization of the electron to the conduction band is the limiting step for e-h pair dissociation); $R_E = n_C/\tau_{\mathrm{tr}}$ is the excitation rate of the Er ion through the proposed mechanism.

Assuming that the excitation rate is negligible, the steady state concentration of the complexes n_C is determined by the equilibrium between the formation rate R_C and the dissociation rate R_D and from Eq. (5) it follows:

$$n_C = \frac{\sigma_p p v_{\mathrm{th}} f(E_T)}{\sigma_p p v_{\mathrm{th}} f(E_T) + e_n} N_{\mathrm{Er}} = \frac{N_{\mathrm{Er}}}{1 + \dfrac{e_n}{\sigma_p p v_{\mathrm{th}} f(E_T)}}. \tag{6}$$

In general $f(E_T)$ will depend on temperature, pump power, and on the energy location of E_T. In the following we will concentrate on the excitation process of the fast decaying component of the impurity-rich samples which we assume to occur through the Er-related level at 0.15 eV from the conduction band. This is in fact the component responsible for the RT luminescence and for the temperature quenching of the luminescence occurring above 200 K. In all the impurity-rich samples we are considering the total donor concentration exceeds $10^{17}/\mathrm{cm}^3$. Therefore, for the level at $E_C - 0.15$ eV, $f(E_T) = 1$ is a reasonable approximation at all temperatures and pump powers. Hence the formation rate of the complexes (R_C) is given by the hole capture rate ($\sigma_p v_{\mathrm{th}} p$). Substituting Eq. (6) in Eq. (4) we obtain

$$I \propto \frac{\tau}{\tau_{\mathrm{rad}}\tau_{\mathrm{tr}}} \frac{N_{\mathrm{Er}}}{1 + \dfrac{e_n}{\sigma_p p v_{\mathrm{th}}}}. \tag{7}$$

The hole concentration $p = G_L \tau_C$, with G_L the optical generation rate of e-h pairs and τ_C the carrier lifetime. The emission rate for an electron captured at the level has been measured by DLTS and is described by $e_n = e_{n_0} e^{-E_T/kT}$, with $E_T = 0.15$ eV and $e_{n_0} = \sigma_n v_{\mathrm{th}} N_C$, where σ_n is the capture cross section for the electron and N_C the effective density of states at the bottom of the conduction band. Hence

$$I \propto \frac{\tau}{\tau_{\mathrm{rad}}\tau_{\mathrm{tr}}} \frac{N_{\mathrm{Er}}}{1 + e_{n_0} e^{-E_T/kT}/\sigma_p G_L \tau_C v_{\mathrm{th}}}$$

$$= \frac{A}{1 + B e^{-0.15\ \mathrm{eV}/kT}}, \tag{8a}$$

where

$$A = \frac{\tau}{\tau_{\mathrm{rad}}\tau_{\mathrm{tr}}} N_{\mathrm{Er}} \tag{8b}$$

and

TABLE I. The values of the parameter B in Eq. (9) used to fit the data in Fig. 4 are reported for the different samples.

Sample	B ($\times 10^3$)
1×10^{20} O/cm^3	7.5
3×10^{19} O/cm^3	20
Cz	50
F doped	35
C doped	80

$$B=\frac{e_{n_0}}{\sigma_p v_{\rm th} G_L \tau_C}. \tag{8c}$$

The intensity I might exhibit a complex temperature dependence since both A and B might depend on temperature through one or more of their factors. However, as a first approximation, we can assume that the dominating contribution to the temperature quenching arises from the exponential term in the denominator of Eq. (8). At 77 K this exponential term is small and hence the PL intensity at this temperature ($I_{77\ \rm K}$) is only given by the term A. Above 77 K the normalized intensity $I_{\rm norm}$ is then given by

$$I_{\rm norm}=\frac{I}{I_{77\ \rm K}}=\frac{1}{1+Be^{-0.15\ \rm eV/kT}}. \tag{9}$$

Fits of Eq. (9) to the data in Fig. 4 are shown as solid lines. It is evident that Eq. (9) has the right functional form to describe the experimental results. In fact $I_{\rm norm}$ has a constant value at low temperatures while at higher temperatures it decreases with an activation energy of 0.15 eV. The temperature at which this temperature quenching sets in depends on the value of the prefactor B. A large value of B corresponds to a large quenching. The B values for the fits in Fig. 4 are reported in Table I. From Table I it is evident that the different quenching behavior for the various impurities and for the different impurity concentrations is directly related to differences in one or more of the factors present in B [see Eq. (8c)]. Let us examine these factors in more detail. Since we performed the measurements reported in Fig. 4 at a fixed pump power, G_L is a constant. The capture cross section for holes (σ_p) and for electrons (σ_n, which enters in the expression of e_{n_0}) to the level related to the Er-impurity complex might be different for the different impurities. This can certainly cause a significant variation in the value of B for the different impurities. Moreover the carrier lifetime τ_C might be different in samples codoped with different impurities. This is expected since DLTS analyses (Fig. 7) show that codoping with different impurities produces a different reduction in the concentration of the Er-related deep levels. Since these deep levels are efficient recombination centers for the carriers, a reduction of these levels would produce an increase in the lifetime τ_C. The increase of τ_C, in turn will produce a reduction in the value of B, and hence a reduced temperature quenching. It is interesting to note that the reduction of the concentration of the deep levels is more marked in O-doped samples which also exhibit the minimum temperature quenching in Fig. 4 (a factor of 30) and hence the lowest B value in Table I. The smallest effect on the deep-level concentration is produced by C which, among the impurity-rich samples, is also the one with the larger quenching in Fig. 4 (a factor 200) and hence the highest B value in Table I. The efficiency of fluorine in both reducing deep-levels concentration and PL temperature quenching lies in between that of O and C.

Finally, it should be noted that, from Eq. (8), a temperature dependence of the PL intensity can derive also from a temperature dependence in the term A. This can arise from a temperature dependence in τ (the decay lifetime) and $\tau_{\rm tr}$ (the transfer time). For example we have demonstrated[8] that in O-doped samples, the slight temperature decrease of the fast decaying component below 200 K is entirely due to a decrease of the decay lifetime due to efficient nonradiative decay routes. Adding this contribution in Eq. (8) would allow also to explain the small reduction in the PL intensity of this component at temperatures below 200 K.

V. CONCLUSIONS

In conclusion, we have studied the Er-impurity interaction and its effect on the 1.54 μm luminescence of Er in crystalline Si. An enhancement of the low temperature Er PL and a reduced temperature quenching have been observed in samples codoped with O, C, or F at concentrations up to 10^{20}/cm^3. Time-decay measurements of the PL intensity, as well as EPR and DLTS analyses demonstrated that, in the presence of the impurity, new well-defined luminescent centers, consisting of Er ions in an impurity-rich environment (Er-impurity complexes), are formed. The formation of these sites results in the introduction of a level in the band gap at 0.15 eV below the conduction band and in the reduction of the concentration of deepest levels. It is proposed that, in impurity-rich samples, Er excitation occurs through the recombination of e-h complexes bound to the level at $E_C-0.15$ eV. The attainment of these impurity-rich sites, which can be pumped through this level, and the reduction of the alternative recombination routes for the free carriers (due to the reduction in the density of deep levels) are responsible for the enhancement of low temperature PL and for the reduced temperature quenching in the presence of the impurities.

ACKNOWLEDGMENTS

We wish to thank Gerlas van den Hoven and Edwin Snoeks for several useful discussions. The expert technical assistance of A. Spada, N. Parasole, and S. Pannitteri is also greatly acknowledged. The work in Catania has been partially supported by the project LES of GNSM and by INFM. The work at FOM was made possible by financial support from NWO, STW, and IOP-ElectroOptics.

[1] H. Ennen, J. Schneider, G. Pomrenke, and A. Axmann, Appl. Phys. Lett. **43**, 943 (1983).
[2] H. Ennen, G. Pomrenke, A. Axmann, K. Eisele, W. Haydl, and J. Schneider, Appl. Phys. Lett. **46**, 381 (1985).
[3] J. Michel, J. L. Benton, R. F. Ferrante, D. C. Jacobson, D. J. Eaglesham, E. A. Fitzgerald, Y. H. Xie, J. M. Poate, and L. C. Kimerling, J. Appl. Phys. **70**, 2672 (1991).
[4] D. L. Adler, D. C. Jacobson, D. J. Eaglesham, M. A. Marcus, J. L. Benton, J. M. Poate, and P. H. Citrin, Appl. Phys. Lett. **61**, 2181 (1992).

[5] P. N. Favennec, H. L'Haridon, D. Moutonnet, M. Salvi, and M. Gauneau, Jpn. J. Appl. Phys. **29**, L524 (1990).
[6] S. Coffa, F. Priolo, G. Franzò, V. Bellani, A. Carnera, and C. Spinella, Phys. Rev. B **48**, 11782 (1993).
[7] F. Priolo, S. Coffa, G. Franzò, C. Spinella, A. Carnera, and V. Bellani, J. Appl. Phys. **74**, 4936 (1993).
[8] S. Coffa, G. Franzò, F. Priolo, A. Polman, and R. Serna, Phys. Rev. B **49**, 16313 (1994).
[9] J. S. Custer, A. Polman, and H. M. van Pinxteren, J. Appl. Phys. **75**, 2809 (1994).
[10] A. Polman, J. S. Custer, E. Snoeks, and G. N. van den Hoven, Appl. Phys. Lett. **62**, 507 (1993).
[11] G. Franzò, F. Priolo, S. Coffa, A. Polman, and A. Carnera, Appl. Phys. Lett. **64**, 2235 (1994).
[12] B. Zheng, J. Michel, F. Y. G. Ren, L. C. Kimerling, D. C. Jacobson, and J. M. Poate, Appl. Phys. Lett. **64**, 2842 (1994).
[13] G. Franzò, F. Priolo, S. Coffa, A. Polman, and A. Carnera, Nucl. Instrum. Methods B **96**, 374 (1995).
[14] S. Lombardo, S. U. Campisano, G. N. van den Hoven, A. Cacciato, and A. Polman, Appl. Phys. Lett. **63**, 1942 (1993).
[15] R. Serna, E. Snoeks, G. N. van den Hoven, and A. Polman, J. Appl. Phys. **75**, 2644 (1994).
[16] A. Polman, G. N. van den Hoven, J. S. Custer, J. H. Shin, R. Serna, and P. F. A. Alkemade, J. Appl. Phys. **77**, 1256 (1995).
[17] S. Lombardo, S. U. Campisano, G. N. van den Hoven, and A. Polman, J. Appl. Phys. **77**, 6504 (1995).
[18] G. N. van den Hoven, A. Polman, S. Lombardo, and S. U. Campisano, J. Appl. Phys. **78**, 2642 (1995).
[19] S. Libertino, S. Coffa, G. Franzò, and F. Priolo, J. Appl. Phys. **78**, 3867 (1995).
[20] M. Tamura and T. Suzuki, Nucl. Instrum. Methods B **39**, 318 (1989); J. R. Liefting, J. S. Custer, and F. W. Saris, Mater. Res. Soc. Symp. Proc. **235**, 179 (1992).
[21] A. Polman, J. S. Custer, E. Snoeks, and G. N. van den Hoven, Nucl. Instrum. Methods B **80**, 653 (1993).
[22] J. I. Pankove and R. J. Feuerstein, Mater. Res. Soc. Symp. Proc. **301**, 287 (1993).
[23] F. Priolo, G. Franzò, S. Coffa, A. Polman, V. Bellani, A. Carnera, and C. Spinella, Mater. Res. Soc. Symp. Proc. **316**, 397 (1994).
[24] A. Abragam and B. Bleaney, *Electron Paramagnetic Resonance of Transition Ions* (Clarendon, Oxford, 1970), p. 325.
[25] M. Baeumler, J. Schneider, F. Kohl, and E. Tomzig, J. Phys. C: Solid State Physics **20**, L963 (1987).
[26] P. B. Klein, F. G. Moore, and H. B. Dietrich, Appl. Phys. Lett. **58**, 502 (1991).
[27] J. D. Kingsley and M. Aven, Phys. Rev. **155**, 235 (1967).
[28] D. Descamps and Y. Merle D'Aubigné, Phys. Lett. **8**, 5 (1964).
[29] M. Needels, M. Schluter, and M. Lannoo, Phys. Rev. B **47**, 15533 (1993).
[30] S. Schmitt-Rink, C. M. Varma, and A. F. J. Levi, Phys. Rev. Lett. **66**, 2782 (1991).
[31] I. N. Yassievich and L. C. Kimerling, Semiconduct. Sci. Technol. **8**, 718 (1993).
[32] H. Przybylinska, G. Hendorfer, M. Bruckner, W. Jantsch, and L. Palmetshofer, Proceedings of the Conference of Rare Earths, Helsinki, 1994 (unpublished).
[33] J. H. Shin, G. N. van den Hoven, and A. Polman, Appl. Phys. Lett. **67**, 377 (1995).